

SrPt₃P: two-band single-gap superconductor

R. Khasanov,^{1,*} A. Amato,¹ P. K. Biswas,¹ H. Luetkens,¹ N. D. Zhigadlo,² and B. Batlogg²

¹Laboratory for Muon Spin Spectroscopy, Paul Scherrer Institute, CH-5232 Villigen PSI, Switzerland

²Laboratory for Solid State Physics, ETH Zurich, 8093 Zurich, Switzerland

The magnetic penetration depth (λ) as a function of applied magnetic field and temperature in SrPt₃P ($T_c \simeq 8.4$ K) was studied by means of muon-spin rotation (μ SR). The dependence of λ^{-2} on temperature suggests the existence of a single s -wave energy gap with the zero-temperature value $\Delta = 1.58(2)$ meV. At the same time λ was found to be strongly field dependent which is the characteristic feature of the nodal gap and/or multi-gap systems. The multi-gap nature of the superconducting state is further confirmed by observation of an upward curvature of the upper critical field. This apparent contradiction would be resolved with SrPt₃P being a two-band superconductor with equal gaps but different coherence lengths within the two Fermi surface sheets.

PACS numbers: 74.72.Gh, 74.25.Jb, 76.75.+i

After the discovery of first Fe-based superconductors enormous efforts were made in order to improve their superconducting properties. The intensive search lead to discovery series of new Fe-based materials (see *e.g.* Ref. 1 for review and references therein) and related compounds such as BaNi₂As₂ [2], SrNi₂As₂ [3], SrPt₂As₂ [4], SrPtAs [5], without Fe and relatively low superconducting transition temperatures T_c 's.

Recently, Takayama *et al.* [6] reported the synthesis of a new family of ternary platinum phosphide superconductors with the chemical formula APt₃P (A = Sr, Ca, and La) and T_c 's of 8.4, 6.6 and 1.5 K, respectively. Theoretical studies on the pairing mechanism in these new compounds achieved partially contradicting results [7, 8]. The authors of Ref. 7 performed first-principles calculations and proposed that superconductivity is caused by the proximity to a dynamical charge-density wave instability, and that a strong spin-orbit coupling leads to exotic pairing in at least LaPt₃P. In contrast, the first principal calculations and Migdal-Eliashberg analysis performed by Subedi *et al.* [8] suggest conventional phonon mediated superconductivity. Also experimentally seemingly contradicting results were obtained. Based on the observation of nonlinear temperature behavior of the Hall resistivity, the authors of Ref. 6 suggest multi-band superconductivity in these new compounds. Note that the presence of two bands crossing the Fermi level was indeed confirmed by ab-initio band structure calculations presented in [7–10]. On the other hand the specific heat data of SrPt₃P were found to be well described within a single band, single s -wave gap approach with the zero-temperature gap value of $\Delta = 1.85$ meV [6].

In this paper we report on the results of muon-spin rotation (μ SR) studies of the magnetic penetration depth (λ) as a function of temperature and magnetic field of the novel superconductor SrPt₃P. Below $T \simeq T_c/2$ the superfluid density ($\rho_s \propto \lambda^{-2}$) becomes temperature independent which is consistent with a fully gapped superconducting state. The full temperature dependence of $\rho_s(T)$ is well described within a single s -wave gap scenario with

the zero-temperature gap value $\Delta = 1.58(2)$ meV. On the other hand, λ was found to increase with increasing magnetic field as is observed in multi-band superconductors or superconductors with nodes in the energy gap. The upper critical field demonstrates a pronounced upward curvature thus pointing to a multi-band nature of the superconducting state of SrPt₃P. Our results indicate that SrPt₃P is a two-band superconductor with equal gaps but different coherence length parameters ξ_i within two Fermi surface sheets.

The sample preparation and the magnetization experiments were performed at the ETH-Zürich. Polycrystalline samples of SrPt₃P were prepared using cubic anvil high-pressure and high-temperature technique. Coarse powders of Sr, Pt, and P elements of high purity (99.99%) were weighed according to the stoichiometric ratio 1:3:1, thoroughly grounded, and enclosed in a boron nitride container, which was placed inside a pyrophyllite cube with a graphite heater. All procedures related to the sample preparation were performed in an argon-filled glove box. In a typical run, a pressure of 2 GPa was applied at room temperature. While keeping the pressure constant, the temperature was ramped up in 2 h to the maximum value of 1050 °C, maintained for 20-40 h, and then decreased to room temperature in 1 h. Afterwards, the pressure was released, and the sample was removed. All high-pressure prepared samples demonstrate large diamagnetic response with the superconducting transition temperature of $\simeq 8.4$ K (see the inset in Fig. 1). The powder x-ray diffraction patterns are consistent with those reported in Ref. 6.

Measurements of the upper critical field B_{c2} were performed using a Quantum Design 14 T PPMS. The temperature dependence of B_{c2} was obtained from zero field-cooled magnetization curves [$M_{ZFC}(T)$] measured in constant magnetic fields ranging from 0.3 mT to 4 T (see Fig. 1). For each particular field the corresponding superconducting transition temperature $T_c(B)$ was taken as an intersect of the linearly extrapolated $M_{ZFC}(T)$ curve in the vicinity of T_c with $M_{ZFC} = 0$ line (see the in-

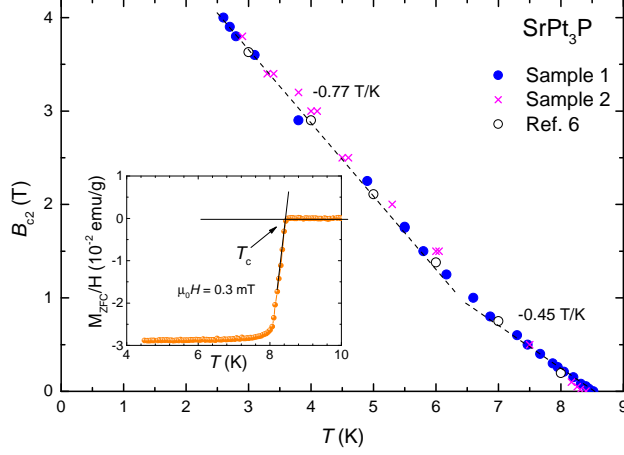


FIG. 1: (Color online) The temperature dependence of the upper critical field B_{c2} of SrPt_3P . The crosses and the circles correspond to two different samples. The solid lines are linear fits of $B_{c2}(T)$ in the vicinity of T_c and for $T \leq 6$ K. Open circles are $B_{c2}(T)$ data points from Ref. 6. The inset shows the temperature dependence of the zero field-cooled magnetization M_{ZFC} measured at $\mu_0 H = 0.3$ mT.

set it Fig. 1). $B_{c2}(T)$ curve exhibits a pronounced upward curvature around $\sim 6 - 6.5$ K. Linear fits of $B_{c2}(T)$ in the vicinity of T_c and for $T \leq 6$ K yield $\text{d}B_{c2}/\text{d}T = -0.45$ and -0.77 T/K, respectively. Open circles correspond to $B_{c2}(T)$ data points from Ref. 6. They are in perfect agreement with our data thus implying that the upturn on $B_{c2}(T)$ reported here is indeed a generic property of SrPt_3P compound. Note that an upward curvature of $B_{c2}(T)$ was also observed previously for a number of materials such as Nb [11, 12], V [11], NbSe₂ [13–15], MgB₂ [16–18], borocarbides and nitrides [19–21], heavy fermion systems [22], various iron-based [23–25] and cuprate superconductors [26, 27] and was often associated with two-band superconductivity.

The temperature and the magnetic field dependence of the magnetic penetration depth λ were obtained from transverse-field (TF) μSR data [28]. The experiments were carried out at the πE1 beam line at the Paul Scherrer Institute (Villigen, Switzerland). The data were analyzed using the free software package MUSRFIT [29]. In a polycrystalline sample the magnetic penetration depth λ can be extracted from the Gaussian muon-spin depolarization rate $\sigma_{sc}(T) \sim \lambda^{-2}$, which reflects the second moment ($\sigma_{sc}^2/\gamma_\mu^2$, γ_μ is the muon gyromagnetic ratio) of the magnetic field distribution due to the flux-line lattice (FLL) in the mixed state [30–32]. The TF- μSR data were analyzed using the asymmetry function:

$$A(t) = A_{sc} \exp[-(\sigma_{sc}^2 + \sigma_n^2)t^2/2] \cos(\gamma_\mu B_{sc}t + \phi) + A_b \exp(-\sigma_b^2 t^2/2) \cos(\gamma_\mu B_b t + \phi) \quad (1)$$

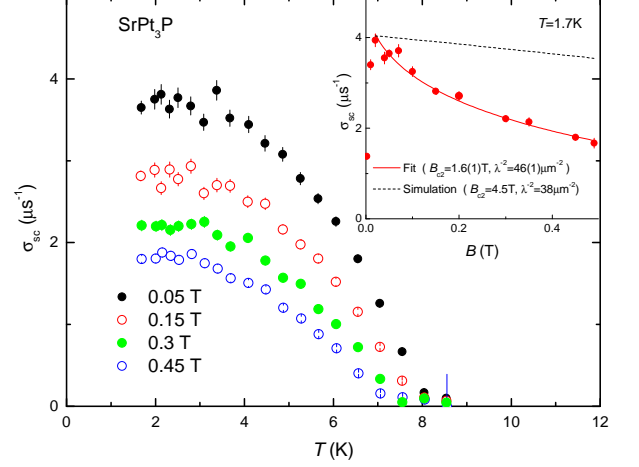


FIG. 2: (Color online) The temperature dependence of the depolarization rate σ_{sc} caused by formation of FLL in SrPt_3P in fields of 0.05, 0.15, 0.3, and 0.45 T. The inset shows the dependence of σ_{sc} on the applied field B at $T = 1.7$ K. The red solid line is the fit of Eq. (2) to $\sigma_{sc}(B)$ data with $\lambda^{-2} = 46(1) \mu\text{m}^{-2}$, $B_{c2} = 1.6(1)$ T. The dashed black line represent $\sigma_{sc}(B)$ as expected for $\lambda^{-2} = 38(1) \mu\text{m}^{-2}$ and $B_{c2} = 4.5$ T obtained in magnetization experiments.

The first term of Eq. (1) represents the response of the superconducting part of the sample. Here A_{sc} denotes the initial asymmetry; σ_{sc} is the Gaussian relaxation rate due to the FLL; σ_n is the contribution to the field distribution arising from the nuclear moment and which is found to be temperature independent, in agreement with the ZF results (not shown); B_{int} is the internal magnetic field sensed by the muons and ϕ is the initial phase of the muon-spin ensemble. The second term with the initial asymmetry A_b , small $\sigma_b < 0.3 \mu\text{s}^{-1}$ and B_b close to the applied field corresponds to the background muons stopping in the cryostat and in nonsuperconducting parts of the sample.

Figure 2 shows the temperature dependence of σ_{sc} in four different fields 0.05, 0.15, 0.3, and 0.45 T. As expected, σ_{sc} is zero in the paramagnetic state and starts to increase below the corresponding $T_c(B)$. Upon lowering T , σ_{sc} increases gradually reflecting the decrease of the penetration depth λ or, correspondingly, the increase of the superfluid density $\rho_s \propto \lambda^{-2}$. The overall decrease of σ_{sc} with increasing applied field is partially caused by the decreased width of the internal field distribution upon approaching B_{c2} . In order to quantify such an effect, one can make use of the numerical Ginzburg-Landau model, developed by Brandt [33]. This model predicts the magnetic field dependence of the second moment of the magnetic field distribution, *i.e.* μSR depolarization rate:

$$\sigma_{sc}[\mu\text{s}^{-1}] = 4.83 \cdot 10^4 (1 - B/B_{c2}) \times$$

$$\times [1 + 1.21(1 - \sqrt{B/B_{c2}})^3] \lambda^{-2} [\text{nm}^{-2}] (2)$$

The insert of Fig. 2 shows the evolution of σ_{sc} at $T = 1.7$ K as a function of the applied magnetic field B . Each data point was obtained after cooling the sample in the corresponding field from above T_c to 1.7 K. Under the assumption of field independent λ the dependence of σ_{sc} on B was analyzed by means of Eq. (2) using the values of the upper critical field B_{c2} as obtained in magnetization experiments [$B_{c2}(1.7 \text{ K}) \simeq 4.5$ T, see Fig. 1]. It is clear from the inset of Fig. 3 that the theoretical $\sigma(B)$ is not in agreement with the data. If B_{c2} is kept as a free parameter in the analysis, the fit yields $B_{c2} = 1.6(1)$ T which is clearly inconsistent with the magnetization data. Therefore one has to conclude that the field independence of λ , which was implicitly assumed in Eq.(2), is not valid (the discussion on field dependence of λ comes later in the paper). The low-temperature value of λ at $B = 0$ [$\lambda(0, B = 0)$] could be estimated by extrapolating two theory lines shown in the inset of Fig. 2 to $B = 0$. This results in $\lambda(0, B = 0) = 155 \pm 10$ nm.

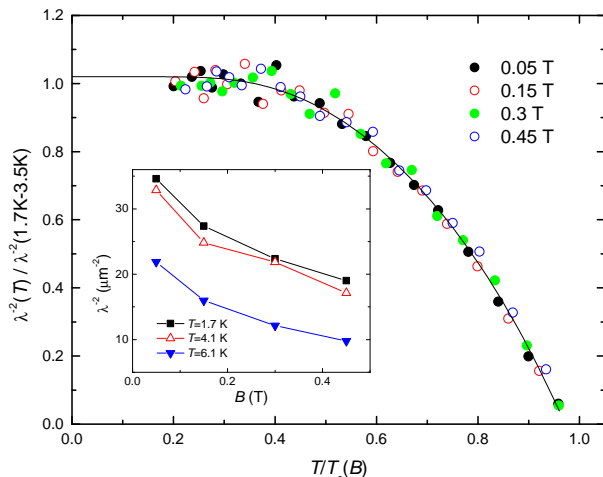


FIG. 3: (Color online) $\lambda^{-2}(T)$ normalized to its value averaged over the temperature range 1.7 – 3.5 K as a function of $T/T_c(B)$. The solid line is the fit by using the weak-coupling BCS model (see Eq. 3). The inset shows the dependence of λ^{-2} on the applied field at $T = 1.7, 4.1$ and 6.1 K.

The temperature dependences of λ^{-2} for $\mu_0 H = 0.05, 0.15, 0.3$, and 0.45 T was obtained from measured $\sigma_{sc}(T)$'s and $B_{c2}(T)$ by using Eq. (2). Figure 3 shows $\lambda^{-2}(T)$ normalized to its value averaged over the temperature range 1.7 – 3.5 K as a function of $T/T_c(B)$. All data curves merge into the single line. The inset of Fig. 3 shows the field dependence of λ^{-2} for $T = 1.7, 4.1$ and 6.1 K.

As a first step we are going to discuss the temperature dependence of λ^{-2} . It is seen that below approximately

one half of T_c , λ^{-2} is temperature independent. The solid line in Fig. 3 represents fit with the weak-coupling BCS model [34]:

$$\frac{\lambda^{-2}(T)}{\lambda^{-2}(0)} = \frac{\rho_s(T)}{\rho_s(0)} = 1 + 2 \int_{\Delta(T)}^{\infty} \left(\frac{\partial f}{\partial E} \right) \frac{E dE}{\sqrt{E^2 - \Delta(T)^2}}. \quad (3)$$

Here $\lambda^{-2}(0)$ and $\rho_s(0)$ are the zero-temperature values of the magnetic penetration depth and the superfluid density, respectively, and $f = [1 + \exp(E/k_B T)]^{-1}$ is the Fermi function. The temperature dependence of the gap is approximated by $\Delta(T)/\Delta(0) = \tanh\{1.82[1.018(T_c/T - 1)]^{0.51}\}$ [35], where $\Delta(0)$ is the maximum gap value at $T = 0$. The fit results in $\Delta(0, B)/k_B T_c(B) = 4.35(4)$, $\lambda^{-2}(T)/\lambda^{-2}(1.7 - 3.5 \text{ K}) = 1.021(6)$, and $T/T_c(B) = 0.972(3)$. For $T_c(B = 0) \simeq 8.4$ K (see Fig. 1) we get $\Delta(T = 0, B = 0) = 1.58(2)$ meV. Note that this value of the superconducting gap is close to $\Delta = 1.85$ meV obtained from zero-field specific heat data by Takayama *et al.* [6].

It is noteworthy that there is no need to introduce more than one gap parameter or to consider more complicated gap symmetry in order to satisfactorily describe $\lambda^{-2}(T)$ data. A fit using two superfluid density components with s -wave gaps Δ_1 and Δ_2 : $\lambda^{-2}(T) = \lambda_1^{-2}(T, \Delta_1) + \lambda_2^{-2}(T, \Delta_2)$, as well as a fit using an anisotropic s -wave gap function result in higher χ^2 than obtained for the simple one gap s -wave model described above. From the analysis of $\lambda^{-2}(T)$ data alone one could therefore conclude that SrPt₃P is a single band s -wave superconductor. Note that the similar conclusion was reached by Takayama *et al.* [6] based on specific heat data. In the following we will suggest that this was a premature conclusion obtained without considering the field dependence of λ .

As follows from the inset in Fig. 3, the field increase from 0.05 up to 0.45 T leads to decrease of λ^{-2} by almost a factor of 2. In a single band s -wave superconductors λ is independent on the magnetic field [31, 35–37]. A dependence of λ on B is expected for superconductors containing nodes in the energy gap or/and multi-gap superconductors [32, 36, 38–40]. In the later case the superfluid density within one series of bands is expected to be suppressed faster by magnetic field than within the others [39, 40].

The single s -wave gap behavior of $\lambda^{-2}(T)$ (see Fig. 3 and the discussion above) and the multi-band features following after the upper critical field B_{c2} and $\lambda^{-2}(B)$ measurements (Fig. 1 and the inset on Fig. 3) allow us to assume that SrPt₃P is a *two-band* superconductor with energy gaps being *equal* within both bands.

Within a two-gap model the deviation from the simple field independence of λ as well as the appearance of upward curvature of the upper critical field could reflect the occurrence of two distinct coherence lengths ξ_1 and ξ_2 for two bands (associated to the corresponding upper critical field values $B_{c2,i} = \phi_0/2\pi\xi_i^2$) [39–44]. For BCS

superconductors the zero-temperature coherence length obeys the relation $\xi \propto \langle v_F \rangle / \Delta$, ($\langle v_F \rangle$ is the averaged value of the Fermi velocity). One could assume, therefore that in SrPt_3P the difference between ξ_1 and ξ_2 could be caused by the different Fermi velocities ($\langle v_{F,1} \rangle \neq \langle v_{F,2} \rangle$), while gaps remain the same ($\Delta_1 = \Delta_2$).

The statement about different $\langle v_F \rangle$'s in two Fermi surface sheets of SrPt_3P is fully confirmed by the calculated band structure [7–10]. According to Refs. 7–10 there are two bands crossing the Fermi level having significantly different v_F 's. The ratio of v_F 's is, *e.g.*, $\simeq 2$ along $\Gamma - X$ and $\sim 3 - 4$ along $\Gamma - Z$ directions of the Brillouin zone. It is worth to note that different Fermi velocities on the different superconducting bands suppose to be a common feature of multi-band superconductors as *e.g.* MgB_2 [45–47], borocarbides [20, 47], Fe-based superconductors [48, 49] *etc.*

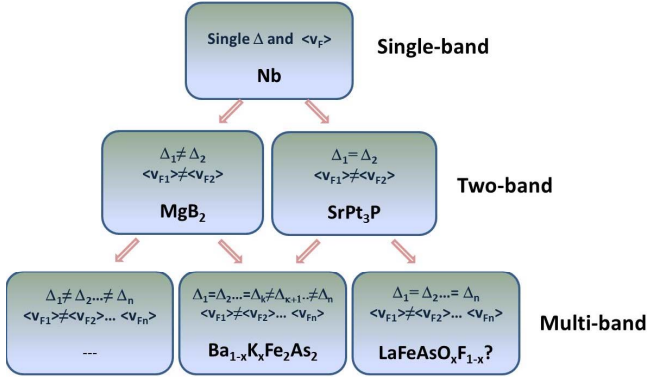


FIG. 4: (Color online) Schematic diagram representing relations between the various types of a single-band, two-band and multi-band superconductors.

Note SrPt_3P studied here is different from the most famous two-band superconductor MgB_2 . In SrPt_3P the charge carriers in both bands suppose to be almost equally coupled to the phonons. Indeed, according to the band structure calculations of Nekrasov *et al.* [9] the carriers in two bands correspond to the relatively *similar* $pd\pi$ antibonding states of Pt(I)-P and Pt(II)-P ions, and are coupled to the *same* low-lying phonon modes confined on the ab plane. In MgB_2 only the σ band carriers are coupled strongly to the so called E_{2g} phonons, while the coupling of both, the σ and the π , bands to the harmonic B_{1g} , A_{2u} , and E_{1u} phonons is negligible [50]. We may conclude, therefore, that MgB_2 and SrPt_3P correspond to two limiting cases of two-band superconductivity with the energy gaps being nonequal ($\Delta_1 \neq \Delta_2$, as in MgB_2) and equal ($\Delta_1 = \Delta_2$, as in SrPt_3P). At the same time SrPt_3P remains the “true” two-band superconductor since, due to nonequal Fermi velocities ($\langle v_{F,1} \rangle \neq \langle v_{F,2} \rangle$), the carriers in various bands “respond” differently to the magnetic field (as shown here

based on $B_{c2}(T)$ and $\lambda(B)$ studies and by Takayama *et al.* [6] based on the observation of nonlinear temperature behavior of the Hall resistivity).

By following the above presented arguments we propose a schematic diagram describing relations between the single-, two-, and the multi-band superconductivity (see Fig. 4). The single-band superconductor has one gap and one averaged over the Fermi surface Fermi velocity ($\langle v_F \rangle$). There are two type of two-band superconductors with energy gaps being equal ($\Delta_1 = \Delta_2$) and nonequal ($\Delta_1 \neq \Delta_2$). Both of these types are characterized, however, by nonequal $\langle v_F \rangle$'s. The “transition” from the two- to the multi-band superconductivity may occur by three different routes. (i) All gaps in all bands crossing the Fermi level are equal ($\Delta_1 = \Delta_2 \dots = \Delta_n$). This is probably the case for the optimally doped $\text{LaFeAsO}_{0.9}\text{F}_{0.1}$ having five Fermi surfaces (as most other Fe-based superconductors, see *e.g.* Ref. 1 and references therein). As shown by Luetkens *et al.* [51] the temperature evolution of the superfluid density of $\text{LaFeAsO}_{0.9}\text{F}_{0.1}$ is well described within the single s -wave gap approach, while λ^{-2} depends strongly on the magnetic field. It should be noted, however that the presence of two distinct gaps in $\text{LaFeAsO}_{0.9}\text{F}_{0.1}$ were reported by Gonnelli *et al.* [52] based on the result of point contact Andreev reflection experiment. (ii) Gaps in some Fermi sheets are equal but in others are not ($\Delta_1 = \Delta_2 \dots = \Delta_k \neq \Delta_{k+1} \dots \neq \Delta_n$). A good example is the optimally doped $\text{Ba}_{1-x}\text{K}_x\text{Fe}_2\text{As}_2$ where three gaps are equal ($\simeq 9$ meV) while the last gap was found to be of approximately eight times smaller ($\simeq 1.1$ meV) [48, 53]. (iii) Gaps in all the Fermi sheets are different ($\Delta_1 \neq \Delta_2 \dots \neq \Delta_n$).

To summaries, the temperature and the magnetic field dependence of the magnetic penetration depth λ in SrPt_3P superconductor ($T_c \simeq 8.4$ K) were studied by means of muon-spin rotation. Below $T \simeq T_c/2$ the superfluid density $\rho_s \propto \lambda^{-2}$ is temperature independent which is consistent with a fully gapped superconducting state. The full $\rho_s(T)$ is well described within the single s -wave gap scenario with the zero-temperature gap value $\Delta = 1.58(2)$ meV. At the same time λ was found to be strongly field dependent which is the characteristic feature of the nodal gap and/or multi-band systems. The multi-band nature of the superconducting state in SrPt_3P was further confirmed by observation of an upward curvature of the upper critical field. To conclude, all above presented results show SrPt_3P to be a two-band superconductor with the equal gaps but different coherence lengths ξ_i associated with the two Fermi surface sheets.

This work was performed at the Swiss Muon Source (μS), Paul Scherrer Institute (PSI, Switzerland).

* Corresponding author: rustem.khasanov@psi.ch

- [1] D.C. Johnston, *Advances in Physics* **59**, 803 (2010).
- [2] E.D. Bauer, F. Ronning, B.L. Scott, and J.D. Thompson, *Phys. Rev. B* **78**, 172504 (2008).
- [3] F. Ronning, N. Kurita, E.D. Bauer, B.L. Scott, T. Park, T. Klimczuk, R. Movshovich, J.D. Thompson, *J. Phys. Condens. Matter*, **20**, 342203 (2008).
- [4] K. Kudo, Y. Nishikubo, M. Nohara, *J. Phys. Soc. Jpn.* **79**, 123710 (2010).
- [5] S. Elgazzar, A.M. Strydom, S.-L. Drechsler, *J. Supercond. Nov. Magn.*, **25**, 1795 (2012).
- [6] T. Takayama, K. Kuwano, D. Hirai, Y. Katsura, A. Yamamoto, and H. Takagi, *Phys. Rev. Lett.* **108**, 237001 (2012).
- [7] H. Chen, X.-F. Xu, C. Cao, and J. Dai, *Phys. Rev. B* **86**, 125116 (2012).
- [8] A. Subedi, L. Ortenzi, and L. Boeri, *Phys. Rev. B* **87**, 144504 (2013).
- [9] I.A. Nekrasov, M.V. Sadovskii, *JETP Letters* **96**, 227 (2012).
- [10] C.-J. Kang, K.-H. Ahn, K.-W. Lee, and B.I. Min, *J. Phys. Soc. Jpn.* **82**, 053703 (2013).
- [11] S.J. Williamson, *Phys. Rev. B* **2**, 3545 (1970).
- [12] H.W. Weber, E. Seidl, C. Laa, E. Schachinger, M. Prohammer, A. Junod, and D. Eckert, *Phys. Rev. B* **44**, 7585 (1991).
- [13] N. Toyota, H. Nakatsuji, K. Noto, A. Hoshi, N. Kobayashi, Y. Muto, and Y. Onodera, *J. Low Temp. Phys.* **25**, 485 (1976).
- [14] D. Sanchez, A. Junod, J. Muller, H. Berger, and F. Levy, *Physica B* **204**, 167 (1995).
- [15] M. Zehetmayer and H.W. Weber, *Phys. Rev. B* **82**, 014524 (2010).
- [16] M. Zehetmayer, M. Eisterer, J. Jun, S.M. Kazakov, J. Karpinski, A. Wisniewski, and H.W. Weber, *Phys. Rev. B* **66**, 052505 (2002).
- [17] A.V. Sologubenko, J. Jun, S.M. Kazakov, J. Karpinski, and H.R. Ott, *Phys. Rev. B* **65**, 180505 (2002).
- [18] L. Lyard, P. Samuely, P. Szabo, T. Klein, C. Marce-nat, L. Paulius, K.H.P. Kim, C.U. Jung, H.-S. Lee, B. Kang, S. Choi, S.-I. Lee, J. Marcus, S. Blanchard, A.G.M. Jansen, U. Welp, G. Karapetrov, and W.K. Kwok, *Phys. Rev. B* **66**, 180502 (2002).
- [19] V. Metlushko, U. Welp, A. Koshelev, I. Aranson, G.W. Crabtree, and P.C. Canfield, *Phys. Rev. Lett.* **79**, 1738 (1997).
- [20] S.V. Shulga, S.-L. Drechsler, G. Fuchs, K.-H. Müller, K. Winzer, M. Heinecke, and K. Krug, *Phys. Rev. Lett.* **80**, 1730 (1998).
- [21] S. Manalo, H. Michor, M. El-Hagary, G. Hilscher, and E. Schachinger, *Phys. Rev. B* **63**, 104508 (2001).
- [22] M.-A. Measson, D. Braithwaite, J. Flouquet, G. Seyfarth, J. P. Brison, E. Lhotel, C. Paulsen, H. Sugawara, and H. Sato, *Phys. Rev. B* **70**, 064516 (2004).
- [23] F. Hunte, J. Jaroszynski, A. Gurevich, D.C. Larbalestier, R. Jin, A.S. Sefat, M.A. McGuire, B.C. Sales, D.K. Christen, D. Mandrus, *Nature* **453**, 903(2008).
- [24] J. Jaroszynski, F. Hunte, L. Balicas, Youn-jung Jo, I. Raicevic, A. Gurevich, D.C. Larbalestier, F.F. Balakirev, L. Fang, P. Cheng, Y. Jia, and H.H. Wen, *Phys. Rev. B* **78**, 174523 (2008).
- [25] S. Ghannadzadeh, J.D. Wright, F.R. Foronda, S.J. Blundell, S.J. Clarke, and P.A. Goddard, *Phys. Rev. B* **89**, 054502 (2014).
- [26] A. Kortyka, R. Puzniak, A. Wisniewski, M. Zehetmayer, H.W. Weber, C.Y. Tang, X. Yao, and K. Conder, *Phys. Rev. B* **82**, 054510 (2010).
- [27] T.B. Charikova, N.G. Shelushinina, G.I. Harus, D.S. Petukhov, V.N. Neverov, and A.A. Ivanov, *Physica C* **488**, 25 (2013).
- [28] A. Yaouanc, P. Dalmas de Réotier, "Muon Spin Rotation, Relaxation and resonance", *Oxford University Press*, (2011).
- [29] A. Suter and B.M. Wojek, *Phys. Procedia* **30**, 69 (2012).
- [30] E.H. Brandt, *Phys. Rev. B* **37**, 2349(R) (1988).
- [31] R. Khasanov, I.L. Landau, C. Baines, F. La Mattina, A. Maisuradze, K. Togano, and H. Keller, *Phys. Rev. B* **73**, 214528 (2006).
- [32] R. Khasanov, A. Shengelaya, A. Maisuradze, F. La Mattina, A. Bussmann-Holder, H. Keller, and K.A. Müller, *Phys. Rev. Lett.* **98**, 057007 (2007).
- [33] E.H. Brandt, *Phys. Rev. B* **68**, 054506 (2003).
- [34] M. Tinkham, "Introduction to Superconductivity", *Krieger Publishing company, Malabar, Florida*, (1975).
- [35] R. Khasanov, D.G. Eshchenko, D. Di Castro, A. Shengelaya, F. La Mattina, A. Maisuradze, C. Baines, H. Luetkens, J. Karpinski, S.M. Kazakov, and H. Keller, *Phys. Rev. B* **72**, 104504 (2005).
- [36] R. Kadono, *J. Phys.: Condens. Matter*, **16**, S4421 (2004).
- [37] R. Khasanov, P.W. Klamut, A. Shengelaya, Z. Bukowski, I.M. Savič, C. Baines, and H. Keller, *Phys. Rev. B* **78**, 014502 (2008).
- [38] M. Angst, D. Di Castro, D.G. Eshchenko, R. Khasanov, S. Kohout, I.M. Savič, A. Shengelaya, S.L. Budko, P.C. Canfield, J. Jun, J. Karpinski, S.M. Kazakov, R.A. Ribeiro, and H. Keller, *Phys. Rev. B* **70**, 224513 (2004).
- [39] A. Bussmann-Holder, R. Khasanov, A. Shengelaya, A. Maisuradze, F. La Mattina, H. Keller, and K.A. Müller, *Europhys. Lett.* **77**, 27002 (2007).
- [40] S. Weyeneth, M. Bendele, R. Puzniak, F. Muranyi, A. Bussmann-Holder, N.D. Zhigadlo, S. Katrych, Z. Bukowski, J. Karpinski, A. Shengelaya, R. Khasanov, and H. Keller, *Europhysics Letters* **91**, 47005, (2010).
- [41] A. Gurevich, *Phys. Rev. B* **67**, 184515 (2003).
- [42] R. Cubitt, M.R. Eskildsen, C.D. Dewhurst, J. Jun, S.M. Kazakov, and J. Karpinski, *Phys. Rev. Lett.* **91**, 047002 (2003).
- [43] S. Serventi, G. Allodi, R. De Renzi, G. Guidi, L. Romanò, P. Manfrinetti, A. Palenzona, Ch. Niedermayer, A. Amato, and Ch. Baines, *Phys. Rev. Lett.* **93**, 217003 (2004).
- [44] M. Mansor and J.P. Carbotte, *Phys. Rev. B* **72**, 024538 (2005).
- [45] H.J. Choi, D. Roundy, H. Sun, M.L. Cohen, and S.G. Louie, *Phys. Rev. B* **66**, 020513 (2002).
- [46] K.D. Belashchenko, M. van Schilfgaarde and V.P. Antropov, *Phys. Rev. B* **64**, 092503 (2001).
- [47] H. Suderow, V.G. Tissen, J.P. Brison, J.L. Martinez, S. Vieira, P. Lejay, S. Lee, and S. Tajima, *Phys. Rev. B* **70**, 134518 (2004).
- [48] D.V. Evtushinsky, D.S. Inosov, V.B. Zabolotnyy, M.S. Viazovska, R. Khasanov, A. Amato, H.-H. Klauss, H. Luetkens, Ch. Niedermayer, G.L. Sun, V. Hinkov, C.T. Lin, A. Varykhalov, A. Koitzsch, M. Knupfer,

- B. Büchner, A.A. Kordyuk, and S.V. Borisenko, *New J. Phys.* **11**, 055069 (2009).
- [49] A. Tamai, A.Y. Ganin, E. Rozbicki, J. Bacsá, W. Meevasana, P.D.C. King, M. Caffio, R. Schaub, S. Margadonna, K. Prassides, M.J. Rosseinsky, and F. Baumberger, *Phys. Rev. Lett.* **104**, 097002 (2010).
- [50] T. Yildirim, O. Gülseren, J.W. Lynn, C.M. Brown, T.J. Udovic, Q. Huang, N. Rogado, K.A. Regan, M.A. Hayward, J.S. Slusky, T. He, M.K. Haas, P. Khalifah, K. Inumaru, and R.J. Cava, *Phys. Rev. Lett.* **87**, 037001 (2001).
- [51] H. Luetkens, H.-H. Klauss, R. Khasanov, A. Amato, R. Klingeler, I. Hellmann, N. Leps, A. Kondrat, C. Hess, A. Kohler, G. Behr, J. Werner, and B. Büchner, *Phys. Rev. Lett.* **101**, 097009 (2008).
- [52] R.S. Gonnelli, D. Daghero, M. Tortello, G.A. Ummarino, V.A. Stepanov, J.S. Kim, and R.K. Kremer, *Phys. Rev. B* **79**, 184526 (2009).
- [53] R. Khasanov, D.V. Evtushinsky, A. Amato, H.-H. Klauss, H. Luetkens, Ch. Niedermayer, B. Büchner, G.L. Sun, C.T. Lin, J.T. Park, D.S. Inosov, and V. Hinkov, *Phys. Rev. Lett.* **102**, 187005 (2009).